Title

PCNA and Msh2-Msh6 Activate an Mlh1-Pms1 Endonuclease Pathway Required for Exo1-Independent Mismatch Repair

Permalink

Journal

ISSN

Authors

Goellner, Eva M
Smith, Catherine E
Campbell, Christopher S
et al.

Publication Date

DOI

Peer reviewed

PCNA and Msh2-Msh6 Activate an Mlh1-Pms1 Endonuclease Pathway Required for Exo1-independent Mismatch Repair

Eva M. Goellner[1], **Catherine E. Smith**[1], **Christopher S. Campbell**[1], **Hans Hombauer**[1,6], **Arshad Desai**[1,3], **Christopher D. Putnam**[1,2], and **Richard D. Kolodner**[1,2,3,4,5]

[1]Ludwig Institute for Cancer Research, University of California, San Diego School of Medicine, La Jolla, CA 92093-0669

[2]Department of Medicine, University of California, San Diego School of Medicine, La Jolla, CA 92093-0669

[3]Department of Cellular and Molecular Medicine, University of California, San Diego School of Medicine, La Jolla, CA 92093-0669

[4]Moores-UCSD Cancer Center, University of California, San Diego School of Medicine, La Jolla, CA 92093-0669

[5]Institute of Genomic Medicine, University of California, San Diego School of Medicine, La Jolla, CA 92093-0669

[6]German Cancer Research Center (DKFZ), 69120 Heidelberg, Germany

Summary

Genetic evidence has implicated multiple pathways in eukaryotic DNA mismatch repair (MMR) downstream of mispair recognition and Mlh1-Pms1 recruitment, including Exonuclease 1 (Exo1) dependent and independent pathways. We identified 14 mutations in *POL30*, which encodes PCNA in *Saccharomyces cerevisiae,* specific to Exo1-independent MMR. The mutations identified affected amino acids at three distinct sites on the PCNA structure. Multiple mutant PCNA proteins had defects either in trimerization and Msh2-Msh6 binding or in activation of the Mlh1-Pms1 endonuclease that initiates excision during MMR. The latter class of mutations led to hyper-accumulation of repair intermediate Mlh1-Pms1 foci and were enhanced by an *msh6* mutation that disrupted the Msh2-Msh6 interaction with PCNA. These results reveal a central role for PCNA in the Exo1-independent MMR pathway and suggest that Msh2-Msh6 localizes PCNA to repair sites after mispair recognition to activate the Mlh1-Pms1 endonuclease for initiating Exo1-dependent repair or for driving progressive excision in Exo1-independent repair.

Introduction

The highly conserved DNA mismatch repair (MMR) pathway is required for genome stability and functions to correct base-base mispairs and small insertion/deletion mispairs that accumulate during normal DNA replication. Defects in MMR genes result in increased mutation rates (Iyer et al., 2006; Kolodner and Marsischky, 1999; Li, 2008) and underlie Lynch syndrome, an inherited cancer predisposition syndrome that leads to an increased risk of a diversity of cancers (de la Chapelle, 2004; Kastrinos and Stoffel, 2013; Peltomaki and Vasen, 1997). In addition, mutations or epigenetic silencing of MMR genes have also been found in many sporadic cancers (Borresen et al., 1995; Kane et al., 1997; Peltomaki, 2003; The Cancer Genome Atlas Network, 2012).

In eukaryotic MMR, mispaired bases are recognized by two partially redundant heterodimers of MutS-related proteins, Msh2-Msh6 and Msh2-Msh3 (Acharya et al., 1996; Drummond et al., 1995; Kolodner and Marsischky, 1999; Marsischky et al., 1996; Palombo et al., 1996). The Msh2-Msh6 complex primarily recognizes base-base mispairs and small insertion/deletion mispairs, whereas the Msh2-Msh3 complex more broadly recognizes insertions/deletions including larger insertions/deletions as well as some single base mispairs (Marsischky et al., 1996; Sia et al., 1997; Srivatsan et al., 2014). The MutL homologue complex Mlh1-Pms1 and, to a lesser extent, the Mlh1-Mlh3 complex are required for MMR along with PCNA, RFC, Polymerase δ, RPA and Exonuclease 1 (Flores-Rozas et al., 2000; Flores-Rozas and Kolodner, 1998; Gu et al., 1998; Johnson et al., 1996; Lin et al., 1998; Liu et al., 2011; Longley et al., 1997; Prolla et al., 1994; Tishkoff et al., 1998; Tishkoff et al., 1997; Xie et al., 1999; Yuan et al., 2004). In addition, there is also some evidence that HMGB1, PARP1 and histone methylation may be partially required for MMR in mammalian cells although the evidence supporting a role for these functions is limited (Li et al., 2013; Liu et al., 2011; Yuan et al., 2004). While a great deal has been learned from biochemical studies of individual MMR proteins and from reconstitution of mispair-dependent excision reactions *in vitro* (Bowen et al., 2013; Constantin et al., 2005; Kadyrov et al., 2009; Pluciennik et al., 2010; Zhang et al., 2005), the *in vivo* mechanisms of eukaryotic MMR downstream of mispair recognition by the MutS homologues, including how mispair excision is appropriately targeted to achieve repair, has not been definitively established.

Exonuclease 1, a 5′ to 3′ exonuclease, is thought to be involved in the excision step of MMR (Genschel et al., 2002; Genschel and Modrich, 2003; Tishkoff et al., 1998; Tishkoff et al., 1997). However, loss of Exo1 in both *Saccharomyces cerevisiae* and mice results in only a weak MMR defect, and *Exo1*$^{-/-}$ mice have a significantly weaker cancer phenotype than observed when other MMR genes are deleted (Amin et al., 2001; Edelmann and Edelmann, 2004; Tishkoff et al., 1997; Wei et al., 2003). These results suggest the presence of at least one Exo1-dependent pathway and at least one redundant Exo1-independent pathway in MMR. Mutations that specifically disrupt the Exo1-independent MMR pathways were identified in a whole genome genetic screen in *S. cerevisiae* supporting the idea that there are redundant Exo1-dependent and -independent MMR pathways (Amin et al., 2001). These mutations affected most of the known MMR genes; however, the majority affected *MLH1* and *PMS1* (Amin et al., 2001), which encode the Mlh1-Pms1 complex that is thought to act

as a PCNA-activated DNA endonuclease that makes nicks in double-stranded DNA that can be substrates for excision during MMR (Gueneau et al., 2013; Kadyrov et al., 2006; Kadyrov et al., 2007; Pluciennik et al., 2010).

A number of mutations that cause defects in MMR have been isolated in *POL30*, which encodes PCNA in *S. cerevisiae*, establishing a critical role for PCNA in MMR (Amin et al., 2001; Lau et al., 2002; Umar et al., 1996). PCNA forms a homotrimer that is required for replication (Krishna et al., 1994; Prelich et al., 1987) and appears to play multiple roles in MMR: (i) the PCNA-Msh6 interaction recruits Msh2-Msh6 to the replication fork, and disruption of this interaction causes a weak mutator phenotype that synergizes with deletion of *EXO1* (Flores-Rozas et al., 2000; Hombauer et al., 2011a); (ii) PCNA loaded by Replication Factor C (RFC) is required to stimulate the Mlh1-Pms1 endonuclease *in vitro* (Kadyrov et al., 2007; Pluciennik et al., 2010); and (iii) PCNA promotes strand resynthesis *in vitro* (Constantin et al., 2005; Umar et al., 1996). Given the multiple roles that PCNA plays in MMR, PCNA could have a role as a central coordinator of MMR.

To understand how PCNA functions in Exo1-independent MMR, we identified and characterized 14 mutations in *POL30* that cause a stronger mutator phenotype in an *exo1* strain than in a wild-type strain. These mutations fell into 2 phenotypic classes, those that altered the interaction between PCNA and Msh2-Msh6 and those that caused defects in the PCNA-mediated activation of the Mlh1-Pms1 endonuclease. All of these mutations caused accumulation of Pms1 foci in strains with wild-type *EXO1*, suggesting that these mutations also perturb the kinetics of Exo1-dependent MMR. Our results suggest the hypothesis that the recruitment or retention of PCNA by Msh2-Msh6 bound to mispairs promotes multiple rounds of PCNA-activated Mlh1-Pms1 endonuclease-mediated cleavage that can compensate for the lack of Exo1 in mispair-promoted DNA resection.

Results

Identification of *pol30* mutations causing defects in Exo1-independent MMR

We generated a plasmid library of PCR-mutagenized versions of *POL30* and used plasmid shuffling to replace a plasmid containing a wild-type copy of *POL30* in an *exo1 pol30* double mutant strain (Lau et al., 2002). Approximately 8,000 colonies were screened for a mutator phenotype resulting in 18 *pol30* alleles that caused a mutator phenotype (Table 1). Of these, 13 were found to cause a mutator phenotype that was dependent on an *exo1* mutation and 1 previously isolated mutation, *pol30-E143K* (mislabelled as *pol30-E143S* in (Amin et al., 2001)), was verified to cause a mutator phenotype that was dependent on an *exo1* mutation (Table 1). Detailed genetic analysis of selected *pol30* alleles reported in this study was performed with mutations present at the *POL30* chromosomal locus.

pol30 mutations that affect Exo1-independent MMR cluster on the protein structure

To gain insight into the 14 *pol30* mutations identified that only cause a strong mutator phenotype in the presence of an *exo1* mutation, the amino acids altered by these mutations were identified on the *S. cerevisiae* PCNA crystal structure (Krishna et al., 1994). The mutations affected amino acids that could be categorized into four groups on the basis of the

protein structure: (i) trimer interface mutations, (ii) the C22-cluster mutations, which affected amino acids at or adjacent to C22 (the residue affected by the *pol30-201* mutation (Lau et al., 2002)), (iii) interdomain connector loop (IDCL)-adjacent mutations, and (iv) unclustered mutations (Figure 1, Table 1). Six of the 13 *pol30* mutations identified in this screen and the previously identified *pol30-E143K* (Amin et al., 2001) were trimer interface mutations that altered amino acids at or near PCNA subunit interfaces (Figure 1 and Figure S1). The *pol30-C81R* mutation was independently isolated as the MMR-defective mutation *pol30-204,* and was shown to encode a protein that destabilized the PCNA trimer and the interaction of PCNA with Msh2-Msh6 (Lau et al., 2002). Three of the mutations were C22-cluster mutations that altered amino acids on the inner face of the PCNA ring either at or near residue C22 (Figure 1 and Figure S1). The *pol30-C22Y* mutation was independently isolated as a MMR-defective mutation (*pol30-201)* (Lau et al., 2002); however, how this mutation causes defects in MMR was not previously understood. The *pol30-K217E* mutation altered the side chain that interacts with the C-terminus of the αA_1 helix and likely affects the conformation of the C22 side chain, suggesting that details of the local conformation may be very important for Exo1-independent MMR (Figure 1). The IDCL-adjacent mutations (*pol30-C30R*, which is a weak allele, and *pol30-L68S*, which is a strong allele) altered amino acids with side chains that are part of a hydrophobic core containing residues of the IDCL, which forms part of the PIP-box binding site, and residues forming the interaction between the interdomain β-sheet and an intersubunit β-sheet (Figure 1 and Figure S1). The remaining 2 mutations were unclustered on the protein structure (Figure 1 and Figure S1); *pol30-F254L* altered a residue adjacent to the glutamine binding site for the PIP-box peptide QxxLxxFF; and *pol30-K13E*, which was also isolated previously (*pol30-114*) (Amin and Holm, 1996), altered a lysine on the inner face of the PCNA ring on the other end of the αA_1 helix, which contains C22. The fact that the altered amino acids tended to cluster on the protein structure would be consistent with the possibility that only a small number of PCNA-based mechanistic defects disrupt Exo1-independent MMR.

Analysis of *pol30* mutations at the endogenous genomic locus

Five trimer interface mutations (*pol30-C81R, pol30-E143K, pol30-D150E, pol30-S152P,* and *pol30-V180D*), the C22-cluster mutations (*pol30-C22Y, pol30-D42V,* and *pol30-K217E*), the IDCL-adjacent mutations (*pol30-C30R* and *pol30-L68S*), and the unclustered mutations (*pol30-K13E* and *pol30-F254L*) were integrated into the *POL30* genomic locus of both wild-type and *exo1* strains (Table 1). The mutator phenotypes caused by all of the mutations, except *pol30-C30R*, were at least partially suppressed in the *EXO1*-containing strain. The different results for the plasmid-borne and integrated *pol30-C30R* allele may result from the very weak phenotype of the plasmid-borne allele, which likely made *EXO1*-complementation difficult to assess (Table 1). Hence, *pol30-C30R* was not extensively studied. Most of the integrated mutations did not cause growth defects at normal growth temperatures (30°C) or sensitivity to heat (37°C) or cold (24°C and 16°C) (Figure S2), and thus are likely not to cause a temperature-dependent cell cycle progression defects. In contrast, *pol30-C30R* caused slow growth at all temperatures except 16°C. The mutation rates caused by a subset of the *pol30* mutations alone or in combination with an *exo1* mutation were determined by fluctuation analysis (Table 2). All of the *pol30* mutations tested caused a synergistic increase in mutation rate in combination with the *exo1* mutation

(all p-values <0.0002, Mann-Whitney test), consistent with the results of the patch test. The *pol30* mutations with effects that were the most specific for the Exo1-independent MMR pathway were *pol30-K217E*, *pol30-K13E*, *pol30-D42V*, *pol30-L68S*, *pol30-F254L*, and *pol30-E143K*. Similar to *pol30-C81R* and *pol30-C22Y* mutations (Lau et al., 2002), the tested mutations (*pol30-E143K*, *pol30-S152P*, *pol30-K217E*, *pol30-D42V*, *pol30-K13E*, *pol30-F254L* and *pol30-L68S*) did not cause a significant increase in the mutation rate of an *msh2* mutant (95% confidence intervals; Table 2), indicating that they do not cause increased misincorporation rates during DNA replication.

pol30 trimer interface mutations cause trimer assembly defects

To probe the molecular defects caused by the *pol30* mutations, we purified representative mutant proteins containing the amino acid substitutions caused by the trimer interface mutations (PCNA-C81R and PCNA-E143K), the C22-cluster mutations (PCNA-C22Y and PCNA-K217E), the IDCL-adjacent mutation (PCNA-L68S), and the ungrouped mutations (PCNA-K13E and PCNA-F254L). As PCNA-C81R and an unrelated trimer interface mutant have trimerization defects (Freudenthal et al., 2009; Lau et al., 2002), we fractionated the mutant PCNA proteins on a size-exclusion column at a concentration of 2.88 μM. Wild-type PCNA had a retention time of 35 minutes, corresponding to a Stokes radius of 49 Å (Figure 2A). The C22-cluster and ungrouped mutant proteins chromatographed similarly to wild-type PCNA. The trimer interface mutant proteins, PCNA-C81R and PCNA-E143K, however, had reduced Stokes radii of 33 Å and 39 Å, respectively (Figure 2A), consistent with destabilization of the trimer. The IDCL-adjacent mutant, PCNA-L68S, also had a reduced Stokes radius of 44 Å potentially indicative of an altered structure mediated by changes in β-sheet packing affecting an intersubunit β-sheet (Figure 1). Given that the *pol30-L68S*, *pol30-C81R* and *pol30-E143K* trimer assembly mutations do not affect cell viability, the proteins resulting from these mutations likely exist in equilibrium with PCNA trimers *in vivo* in order for PCNA to be functional. Consistent with this, the elution profile of PCNA-C81R was similar to that of wild-type PCNA at higher concentrations (23 μM; data not shown).

pol30 trimer interface mutations affect binding of PCNA to Msh2-Msh6

PCNA binds Msh2-Msh6 through a PIP-box motif at the N-terminus of Msh6 (Flores-Rozas et al., 2000), and this interaction has been previously shown to be compromised by the trimer interface mutation *pol30-C81R in vitro* (Lau et al., 2002) and *in vivo* (Hombauer et al., 2011a). We therefore tested the interactions of the mutant PCNA proteins with Msh2-Msh6 by monitoring binding of Msh2-Msh6 to immobilized PCNA using surface plasmon resonance (SPR). The Msh2-Msh6 binding to the PCNA trimer interface mutants was reduced compared with wild-type PCNA (Figure 2B, S3). PCNA-L68S, which had a slightly reduced Stokes radius, also showed slightly reduced Msh2-Msh6 binding. Additionally, the PCNA-F254L mutant, which had no defects in trimer stability but had an amino acid substitution adjacent to the PIP-box binding site, showed slightly reduced Msh2-Msh6 binding. In contrast, the C22-cluster mutant proteins PCNA-C22Y and PCNA-K217E and the unclustered mutant, PCNA-K13E, bound to Msh2-Msh6 at levels equal to or greater than wild-type PCNA (Figure 2B). The basis for the increased binding of PCNA-K13E to Msh2-Msh6 is not clear, but may suggest some type of altered interaction with Msh2-Msh6.

Together these results support previous data showing a Msh2-Msh6 binding defect with PCNA-C81R and extend this observation to other trimerization-perturbing PCNA mutant proteins.

PCNA-C22-cluster mutations and PCNA-K13E cause defects in activating the Mlh1-Pms1 endonuclease

PCNA activates the Mlh1-Pms1 endonuclease activity *in vitro* when loaded onto a supercoiled plasmid by RFC (Kadyrov et al., 2006; Kadyrov et al., 2007; Pluciennik et al., 2010). We therefore tested the ability of the purified mutant PCNA proteins to activate Mlh1-Pms1 endonuclease activity. The trimer interface mutants PCNA-C81R and PCNA-E143K, the IDCL-adjacent mutant PCNA-L68S, and the unclustered mutant PCNA-F254L activated Mlh1-Pms1 endonuclease activity to the same levels as wild-type PCNA (Figure 2C). In contrast, the C22-cluster mutant proteins, PCNA-C22Y and PCNA-K217E, and the unclustered mutant protein, PCNA-K13E, had substantial defects in activating Mlh1-Pms1 endonuclease activity (Figure 2C); the defect seen for PCNA-C22Y is consistent with a previous suggestion that this mutant protein had a defect in a step of MMR downstream of mispair recognition by Msh2-Msh6 or Msh2-Msh3 (Lau et al., 2002). The mutant proteins exhibiting reduced Mlh1-Pms1 activation all had amino acid substitutions affecting residues on the inner surface of the PCNA ring whereas none of these mutant proteins had trimerization defects or Msh2-Msh6 binding defects.

pol30 mutations with defects in activating Mlh1-Pms1 endonuclease activity lead to accumulation of MMR intermediates even in the presence of Exo1

Live cell imaging of tagged MMR proteins recently revealed that Mlh1-Pms1 foci form as an intermediate during normal MMR (Hombauer et al., 2011a). Genetic manipulations that disrupted or delayed MMR at steps downstream of Mlh1-Pms1 recruitment (such as an *exo1* mutation) or increased the frequency of misincorporation errors during DNA replication increased the frequency of cells with Mlh1-Pms1 foci, consistent with the view that these foci are repair intermediates (Hombauer et al., 2011a). We therefore monitored the formation of Pms1-4xGFP foci in strains with a wild-type copy of *EXO1* and the *pol30* mutation of interest integrated at the genomic locus. Cells with *pol30* mutations affecting trimer assembly and Msh2-Msh6 binding (*pol30-C81R, pol30-E143K,* and *pol30-L68*S, which also causes slight defects in trimer assembly and Msh2-Msh6 binding but is not located at the trimer interface), had elevated levels of Pms1 foci (23–58% of cells had Pms1 foci; Figure 3). Cells with *pol30* mutations affecting activation of Mlh1-Pms1 endonuclease activity (*pol30-C22Y, pol30-K217E*, and *pol30-K13E*) had an even greater increase in Pms1 foci (80-100% of cells had Pms1 foci; Figure 3). The *pol30-D42V* mutation caused only a very modest increase in the percentage of cells with Pms1 foci, unlike other members of the C22-cluster; this result was consistent with the weaker mutator phenotype caused by the *pol30-D42V* mutation compared to the other C22-cluster mutations (Table 1). Similarly, the *pol30-F254L* mutation that causes a relatively weak mutator phenotype also caused correspondingly low levels of Pms1 foci. The increased levels of Pms1 foci observed with the *pol30-C22Y* mutation were eliminated by an *msh2* mutation, consistent with previous results showing that mispair recognition by Msh2-Msh6 or Msh2-Msh3 is required for the accumulation of Pms1 repair intermediate foci (Hombauer et al., 2011a) (Figure 3). The

increased levels of Pms1 foci observed here were seen in strains with wild-type *EXO1*, despite the fact that wild-type strains containing these *pol30* mutations are largely MMR-proficient (Tables 1, 2). These results are consistent with a slower turnover of MMR intermediates in strains with these *pol30* mutations even in the presence of *EXO1*.

pol30 mutations that affect the trimer interfaces are dominant

To further characterize the different groups of *pol30* mutations, we tested the effects of expressing the mutant proteins on low-copy number plasmids in *EXO1* and *exo1* strains. All of the plasmid-borne trimer interface mutations caused a dominant mutator phenotype in *EXO1* and *exo1* strains that contained a wild-type copy of *POL30* at its genomic locus, whereas none of the mutations tested from the other groups caused a dominant mutator phenotype (Figure S4). We also tested whether overexpression of the *pol30* mutations on high-copy plasmids in the *exo1* strain in the absence of wild-type *POL30* caused reduced mutator phenotypes compared to when the *pol30* mutations were expressed on a low-copy ARS-CEN plasmid (previously measured in Table 1). Overexpression of the trimer interface mutations (*pol30-C81R* and *pol30-E143K*), the C22-cluster mutations (*pol30-C22Y*, *pol30-K217E*, and *pol30-D42V*), the IDCL-adjacent mutation (*pol30-L68S*) and the unclustered mutations (*pol30-K13E* and *pol30-F254L*) did not cause a reduced mutator phenotype compared to that caused by expression of the same mutation on a low-copy plasmid (Figure S5). Therefore, the *pol30* trimer interface mutations are dominant and the other *pol30* mutations are recessive.

Disruption of Msh2-Msh6 binding to PCNA is synergistic with *pol30* mutations that disrupt Mlh1-Pms1 endonuclease activation

The *pol30* mutations fell into four groups on the basis of the crystal structure, but characterization of the mutant proteins identified two major functional classes; mutations that affect the activation of the Mlh1-Pms1 endonuclease *in vitro* and mutations that reduce PCNA trimer stability and binding of PCNA to Msh2-Msh6. If these functional classes of mutations cause defects in different steps of the Exo1-independent repair pathway, we would predict there would be differences in the interactions between these mutations and mutations in *MSH6* that eliminate the interaction between Msh6 and PCNA. Specifically, a *pol30* mutation causing a partial defect in activation of the Mlh1-Pms1 endonuclease would be predicted to cause a synergistic increase in mutation rate when PCNA could no longer be recruited or retained by Msh2-Msh6. In contrast, a *pol30* mutation that causes defects in PCNA trimerization and the interaction with Msh2-Msh6 would be predicted to not cause a synergistic increase in mutation rate under the same conditions. To test this we combined different *pol30* mutations located at the chromosomal *POL30* locus with a chromosomal *msh6 2-50* allele, which deletes the N-terminal residues containing the Msh6 PIP box, disrupts the Msh6-PCNA interaction, and synergizes with an *exo1* mutation (Hombauer et al., 2011a; Shell et al., 2007). These experiments were performed in a strain containing wild-type *EXO1* and an *msh3* mutation, the latter of which eliminates complications due to Msh2-Msh3 dependent MMR. We found that the trimer interface mutation *pol30-E143K* that appears to cause a defect in the interaction between PCNA and Msh2-Msh6 caused a small increase in mutation rate in the *msh6 2-50 msh3* mutant, whereas the *pol30* mutations that disrupted the activation of the Mlh1-Pms1 endonuclease (*pol30-K217E* and

pol30-K13E) caused much larger synergistic increases in mutation rate when combined with the *msh6 2-50 msh3* double mutation (Table 3). The two other mutations tested (*pol30-F254L, pol30-L68S*) had differing effects. The *pol30-F254L* (unclustered) mutation did not synergize with the *msh6 2-50 msh3* double mutation, which would be consistent with causing a weak defect in interaction between PCNA and Msh2-Msh6. The *pol30-L68S* (IDLC-adjacent) mutation, on the other hand, did synergize with the *msh6 2-50 msh3* double mutation, but not to the same extent as seen with the Mlh1-Pms1 activation-defective mutations. Given the differences between *pol30-L68S* and the trimer interface mutations and the fact that the *pol30-L68S* single mutation caused a larger increase in mutation rate than any of the other mutations tested, these data suggest that this mutation belongs to an additional class of *pol30* mutations or that this mutation results in a protein with a weak defect in activation of the Mlh1-Pms1 endonuclease that is not readily detected by the *in vitro* assays.

Discussion

We performed a gene-specific screen for *pol30* mutations that cause a mutator phenotype that is dependent on an *exo1* mutation. This screen identified 14 *pol30* mutations affecting single amino acids that could be assigned to four groups based on the *S. cerevisiae* PCNA structure (Krishna et al., 1994) and divided into 2 major functional classes by biochemical and genetic characterization: 1) mutants with defects in activating the Mlh1-Pms1 endonuclease (the C22-cluster mutants and PCNA-K13E) and 2) mutants with partial defects in PCNA trimerization and/or in interacting with Msh2-Msh6 (trimer interface mutants). The proteins resulting from the other mutations did not cleanly fall into either of these major functional classes. PCNA-F254L (unclustered) had an amino acid substitution adjacent to the PIP-box binding site, but differed from the second class by exhibiting only weak defects in Msh2-Msh6 binding and no other biochemical defect. PCNA-L68S (IDLC-adjacent) activated Mlh1-Pms1, but had far weaker defects in trimerization and Msh2-Msh6 binding than the trimer interface mutations. The *pol30-L68S* mutation also synergized with the *msh6 2-50* mutation and resulted in a large increase of Mlh1-Pms1 foci, suggesting that the PCNA-L68S protein may have additional biochemical defects.

Other mutations also cause a mutator phenotype that synergize with loss of the Exo1-dependent MMR pathway(s). Most of these mutations appear to fall into two major categories that mirror the major categories of the *pol30* mutations identified here: 1) mutations affecting the Mlh1-Pms1 complex (Amin et al., 2001; Tran et al., 2001) as well as loss-of-function mutations in *PMS1* and *MLH1* that have a partial dominant MMR defect in *exo1* mutants (Smith et al., 2013); and 2) mutations in *MSH6* affecting the interaction between Msh2-Msh6 and PCNA (Hombauer et al., 2011a). These classes of mutations cause distinct biochemical defects but are similar in terms of causing a synergistic increase in mutation rate when combined with a deletion of *EXO1* and, in those cases tested, causing the accumulation of Pms1 repair intermediate foci in cells when Exo1 is expressed. This suggests both classes of mutations affect the kinetics of the MMR reaction that occurs in the presence of Exo1 and that the mechanistic differences between the Exo1-dependent and Exo1-independent pathways are in steps downstream of mispair recognition by Msh2-Msh6 or Msh2-Msh3 and recruitment of Mlh1-Pms1.

The *exo1* mutation synergizing mutations affecting the Mlh1-Pms1 endonuclease include mutations in the genes encoding PCNA and Mlh1-Pms1 (Figure 2C and (Smith et al., 2013)). PCNA activates the Mlh1-Pms1 endonuclease *in vitro* (Kadyrov et al., 2006; Kadyrov et al., 2007; Pluciennik et al., 2010), and the C22-cluster *pol30* mutations (*pol30-C22Y* and *pol30-K217E*) and the unclustered *pol30-K13E* mutation are the first *pol30* mutations identified that cause defects in activating the Mlh1-Pms1 endonuclease. The effect of these mutations provides the first evidence that PCNA activation of Mlh1-Pms1 in MMR occurs *in vivo* as well as *in vitro* and that disruption of this activation causes a defect in MMR. The *pol30* mutations identified here could function by directly altering an Mlh1-Pms1 interaction surface on PCNA. In this regard, the structure of PCNA-C22Y revealed only modest and localized changes (Dieckman et al., 2013), arguing against large-scale structural changes. Alternatively, the *pol30* mutations could function by a more indirect effect involving PCNA loading or proper association with DNA. The PCNA-K217A mutant protein has 2-fold reduced clamp opening (Zhou and Hingorani, 2012) and an alteration of the positive charge on the inner surface of PCNA could affect how PCNA interacts with DNA (Ivanov et al., 2006), although the *in vivo* effects of such alterations are unknown. Regardless, none of the C22-cluster mutations caused cold-sensitivity or inviability (Figure S2) and the *pol30-C22Y* mutation did not alter cell cycle progression at either 16°C or 30°C (Lau et al., 2002) suggesting the C22-cluster mutations are unlikely to cause substantial clamp loading defects.

The *pol30-C22*-cluster and *pol30-K13E* mutations largely phenocopy the dominant effects of plasmid-encoded endonuclease active site *mlh1* and *pms1* mutations (Smith et al., 2013). Both classes of mutations synergize with an *exo1* mutation and cause an increased accumulation of Pms1-4xGFP foci intermediates (Table 2, Figure 3, (Smith et al., 2013)). The interesting distinction is that the nuclease-deficient *mlh1* and *pms1* mutations are loss-of-function mutations that cause complete MMR defects, but are weakly dominant and synergize with an *exo1* mutation in the presence of the wild-type *MLH1* and *PMS1* genes, respectively (Smith et al., 2013). In contrast, the *pol30* mutations disrupting the endonuclease activation cause low mutation rates as single mutations (Table 2). Unless the previously described *mlh1* and *pms1* active site mutations also cause other defects in the Mlh1-Pms1 complex, it seems likely that the *pol30* mutations studied here must only cause partial defects in Mlh1-Pms1 endonuclease activity, consistent with the idea that greater levels of Mlh1-Pms1 endonuclease activity are required for MMR in the absence of Exo1 than in the presence of Exo1 (Figure 4, (Smith et al., 2013)).

The *exo1*-synergizing mutations affecting the PCNA interaction with Msh2-Msh6 include *msh6 2-50 and msh6-F33AF34A,* both of which disrupt the Msh2-Msh6 interaction with PCNA (Hombauer et al., 2011a; Shell et al., 2007), and *pol30* mutations that cause partial trimerization defects by affecting amino acids at the trimer interface (*pol30-C81R, pol30-E143K*) or elsewhere in PCNA (*pol30-L68S*). We showed that the trimer-interface mutants that were novel (*pol30-S152P*, *pol30-D150E* and *pol30-V180D*), re-identified (*pol30-Y114H*, *pol30-S177P*), and previously identified (*pol30-E143K*) synergized with a deletion of *EXO1*. How these trimerization defects affect Msh2-Msh6 binding is unclear but may result from the fact that the IDCL, which contains part of the PIP-box binding site, starts at

the end of βI_1, which is part of the trimer interface (Figure 1). Consistent with the requirement that these mutant PCNAs must be functional, the PCNA-C81R structure revealed only small changes at the interface (Dieckman et al., 2013), potentially reflecting the ability of PCNA-C81R to trimerize at high concentrations. Furthermore, PCNA-C81R did not show alternative assemblies like another mutant PCNA resulting from a trimer interface mutation, PCNA-E113G (Freudenthal et al., 2009), which has not been tested for its effect on MMR. Interestingly, PCNA-C81R appeared to form an aberrant complex with Msh2-Msh6 and an oligonucleotide duplex containing a GT mispair (Dieckman et al., 2013). Alteration of the PCNA interaction with Msh2-Msh6 by *msh6-PIP-box* and *pol30* trimer interface mutations synergizes with an *exo1 pol30*, and Pms1 foci form at normal levels in *msh6-PIP box* mutants but form at higher levels in *pol30* trimer interface mutations. These facts are consistent with the *pol30* trimer interface mutants having additional biochemical defects beyond altering the Msh2-Msh6 interaction and are consistent with a role for the PCNA-Msh2-Msh6 interaction downstream of Mlh1-Pms1 recruitment.

We propose a hypothesis in which both classes of *pol30* mutations that synergize with loss of *EXO1* result in the same mechanistic defect: loss of efficient activation of the Mlh1-Pms1 endonuclease (Figure 4). Msh2-Msh6 (or Msh2-Msh3) is required for mismatch recognition and recruitment of Mlh1-Pms1 (Kolodner and Marsischky, 1999). It has not been definitively determined how the newly synthesized DNA strands are identified during MMR, although it has been shown that signals generated during S-phase are required for MMR (Hombauer et al., 2011b). These signals potentially include PCNA retained on DNA during DNA replication or nicks in the newly synthesized DNA strands that are potentially sites for RFC-mediated loading of PCNA (Hombauer et al., 2011b; Pluciennik et al., 2010). However the newly synthesized DNA strand is identified, nicks in DNA generated by the endonuclease activity of Mlh1-Pms1 are likely required for both Exo1-independent MMR and Exo1-dependent MMR as *pms1* active site mutations cause complete defects in MMR (Deschenes et al., 2007; Erdeniz et al., 2007; Kadyrov et al., 2007; Smith et al., 2013). The Mlh1-Pms1 endonuclease is generally required for MMR even though nicks left in the lagging strand during DNA replication appear to preferentially target Exo1-dependent MMR to repair lagging DNA strand replication errors (Hombauer et al., 2011a; Liberti et al., 2013). Our hypothesis proposes that the Exo1-independent pathway requires multiple rounds of incision by Mlh1-Pms1, possibly followed by DNA polymerase δ-mediated strand displacement (Kadyrov et al., 2009) or DNA polymerase-associated editing exonucleases (Tran et al., 1999), and hence is more sensitive to poisoning by nuclease-deficient versions of Mlh1-Pms1 (Smith et al., 2013), or, as shown here, mutant forms of PCNA with defects in activating Mlh1-Pms1, and that the ability of Exo1 to catalyse long excision tracts (Bowen et al., 2013) during MMR substitutes for multiple rounds of incision by Mlh1-Pms1 during Exo1-dependent MMR (Figure 4). In most proposed MMR mechanisms Msh2-Msh6 has not been implicated in any step after Mlh1-Pms1 recruitment; however, the Msh2-Msh6 2-50 mutant and the PCNA mutants with reduced Msh2-Msh6 binding have defects in Exo1-independent MMR, suggesting that Msh2-Msh6 influences the downstream mispair excision step by either recruiting or retaining PCNA at sites of repair through the N-terminal unstructured tether that contains the PIP-box motif (Shell et al., 2007). This recruited or retained PCNA is then available for activation of Mlh1-Pms1 and is likely more important in

Exo1-independent reactions involving multiple rounds of Mlh1-Pms1 incision, but probably also plays a role in Exo1-dependent MMR reactions as evidenced by increased Pms1 foci caused by the *pol30-C81R* and *pol30-E143K* trimer interface mutations in strains with wild-type *EXO1* (Figure 3).

In support of this hypothesis, the *msh6 2-50* mutation strongly synergizes with *pol30* mutations that disrupt the activation of the Mlh1-Pms1 endonuclease, whereas the *msh6 2-50* mutation in combination with a *pol30* mutation that alters interactions between PCNA and Msh2-Msh6 results in a mutation rate that is only slightly higher compared to the mutation rate caused by the *msh6 2-50* mutation alone. These results confirm that the trimer interface mutations impart their mutator phenotype primarily through alteration of the interaction between PCNA and Msh2-Msh6. Furthermore, these data highlight that the *pol30* mutations that cause defects in the activation of the Mlh1-Pms1 endonuclease are only partially defective (30% of wild-type activity compared to 5% of wild-type activity for Mlh1-Pms1 with no PCNA) and can be further enhanced by loss of PCNA recruitment resulting in a high mutation rate even in the presence of *EXO1*. Our data support the hypothesis that Msh2-Msh6 binding and recruitment/retention of PCNA is required for efficient activation of the Mlh1-Pms1 endonuclease, and suggest that Msh2-Msh6 plays an important role in promoting MMR downstream of mispair recognition and Mlh1-Pms1 recruitment through this interaction.

Experimental Procedures

S. cerevisiae strains

All *S. cerevisiae* strains in this study (Table S1) were derived from the S288C background and propagated using standard media.

Mutation screen

A plasmid library of mutations in the *POL30* gene was generated by PCR amplification mutagenesis followed by transformation into the *pol30 exo1* strain RDKY8260 using the plasmid shuffle technique and the mutations screened to identify those causing *exo1*-dependent mutator phenotypes as described (Amin et al., 2001; Lau et al., 2002).

Protein purification and biochemical studies

Wild-type PCNA, Msh2-Msh6, Mlh1-Pms1 and RFC- 1N were purified as reported (Bowen et al., 2013) and mutant PCNA proteins (PCNA-C81R, PCNA-E143K, PCNA-C22Y, PCNA-K217E, PCNA-K13E, PCNA-L68S and PCNA-F254L) were similarly overexpressed using plasmids pRDK931-pRDK932 and pRDK1763-pRDK1767 (Table S2) and purified. Purified PCNA was chromatographed on a Sepax SRT SEC-300 sepharose size exclusion column. The PCNA interaction with Msh2-Msh6 was determined using SPR with a BiacoreT100 as described (Shell et al., 2007). The *in vitro* Mlh1-Pms1 endonuclease assays were performed exactly as described (Smith et al., 2013).

Cell imaging studies

Imaging and analysis of Mlh1-Pms1 GFP foci was carried out as described using 2 independent strain isolates in each experiment (Hombauer et al., 2011a; Smith et al., 2013).

Statistical analysis

95 % confidence intervals were calculated for all fluctuation tests. Mann-Whitney tests were performed to report the two-tailed p-values for comparisons between rates (http://vassarstats.net/utest.html).

Supplementary Material

Refer to Web version on PubMed Central for supplementary material.

Acknowledgments

References

Acharya S, Wilson T, Gradia S, Kane MF, Guerrette S, Marsischky GT, Kolodner R, Fishel R. hMSH2 forms specific mispair-binding complexes with hMSH3 and hMSH6. Proceedings of the National Academy of Sciences of the United States of America. 1996; 93:13629–13634. [PubMed: 8942985]

Amin NS, Holm C. In vivo analysis reveals that the interdomain region of the yeast proliferating cell nuclear antigen is important for DNA replication and DNA repair. Genetics. 1996; 144:479–493. [PubMed: 8889514]

Amin NS, Nguyen MN, Oh S, Kolodner RD. exo1-Dependent mutator mutations: model system for studying functional interactions in mismatch repair. Molecular and cellular biology. 2001; 21:5142–5155. [PubMed: 11438669]

Borresen AL, Lothe RA, Meling GI, Lystad S, Morrison P, Lipford J, Kane MF, Rognum TO, Kolodner RD. Somatic mutations in the hMSH2 gene in microsatellite unstable colorectal carcinomas. Human molecular genetics. 1995; 4:2065–2072. [PubMed: 8589682]

Bowen N, Smith CE, Srivatsan A, Willcox S, Griffith JD, Kolodner RD. Reconstitution of long and short patch mismatch repair reactions using Saccharomyces cerevisiae proteins. Proceedings of the National Academy of Sciences of the United States of America. 2013; 110:18472–18477. [PubMed: 24187148]

Chen C, Merrill BJ, Lau PJ, Holm C, Kolodner RD. Saccharomyces cerevisiae pol30 (proliferating cell nuclear antigen) mutations impair replication fidelity and mismatch repair. Molecular and cellular biology. 1999; 19:7801–7815. [PubMed: 10523669]

Constantin N, Dzantiev L, Kadyrov FA, Modrich P. Human mismatch repair: reconstitution of a nick-directed bidirectional reaction. The Journal of biological chemistry. 2005; 280:39752–39761. [PubMed: 16188885]

de la Chapelle A. Genetic predisposition to colorectal cancer. Nature reviews Cancer. 2004; 4:769–780.

Deschenes SM, Tomer G, Nguyen M, Erdeniz N, Juba NC, Sepulveda N, Pisani JE, Liskay RM. The E705K mutation in hPMS2 exerts recessive, not dominant, effects on mismatch repair. Cancer letters. 2007; 249:148–156. [PubMed: 17029773]

Dieckman LM, Boehm EM, Hingorani MM, Washington MT. Distinct structural alterations in proliferating cell nuclear antigen block DNA mismatch repair. Biochemistry. 2013; 52:5611–5619. [PubMed: 23869605]

Drummond JT, Li GM, Longley MJ, Modrich P. Isolation of an hMSH2-p160 heterodimer that restores DNA mismatch repair to tumor cells. Science (New York, NY. 1995; 268:1909–1912.

Edelmann L, Edelmann W. Loss of DNA mismatch repair function and cancer predisposition in the mouse: animal models for human hereditary nonpolyposis colorectal cancer. American journal of medical genetics Part C, Seminars in medical genetics. 2004; 129C:91–99.

Erdeniz N, Nguyen M, Deschenes SM, Liskay RM. Mutations affecting a putative MutLalpha endonuclease motif impact multiple mismatch repair functions. DNA repair. 2007; 6:1463–1470. [PubMed: 17567544]

Flores-Rozas H, Clark D, Kolodner RD. Proliferating cell nuclear antigen and Msh2p-Msh6p interact to form an active mispair recognition complex. Nature genetics. 2000; 26:375–378. [PubMed: 11062484]

Flores-Rozas H, Kolodner RD. The Saccharomyces cerevisiae MLH3 gene functions in MSH3-dependent suppression of frameshift mutations. Proceedings of the National Academy of Sciences of the United States of America. 1998; 95:12404–12409. [PubMed: 9770499]

Freudenthal BD, Gakhar L, Ramaswamy S, Washington MT. A charged residue at the subunit interface of PCNA promotes trimer formation by destabilizing alternate subunit interactions. Acta crystallographica Section D, Biological crystallography. 2009; 65:560–566.

Genschel J, Bazemore LR, Modrich P. Human exonuclease I is required for 5′ and 3′ mismatch repair. The Journal of biological chemistry. 2002; 277:13302–13311. [PubMed: 11809771]

Genschel J, Modrich P. Mechanism of 5′-directed excision in human mismatch repair. Molecular cell. 2003; 12:1077–1086. [PubMed: 14636568]

Gu L, Hong Y, McCulloch S, Watanabe H, Li GM. ATP-dependent interaction of human mismatch repair proteins and dual role of PCNA in mismatch repair. Nucleic acids research. 1998; 26:1173–1178. [PubMed: 9469823]

Gueneau E, Dherin C, Legrand P, Tellier-Lebegue C, Gilquin B, Bonnesoeur P, Londino F, Quemener C, Le Du MH, Marquez JA, et al. Structure of the MutLalpha C-terminal domain reveals how Mlh1 contributes to Pms1 endonuclease site. Nature structural & molecular biology. 2013; 20:461–468.

Hombauer H, Campbell CS, Smith CE, Desai A, Kolodner RD. Visualization of eukaryotic DNA mismatch repair reveals distinct recognition and repair intermediates. Cell. 2011a; 147:1040–1053. [PubMed: 22118461]

Hombauer H, Srivatsan A, Putnam CD, Kolodner RD. Mismatch repair, but not heteroduplex rejection, is temporally coupled to DNA replication. Science (New York, NY. 2011b; 334:1713–1716.

Ivanov I, Chapados BR, McCammon JA, Tainer JA. Proliferating cell nuclear antigen loaded onto double-stranded DNA: dynamics, minor groove interactions and functional implications. Nucleic acids research. 2006; 34:6023–6033. [PubMed: 17071716]

Iyer RR, Pluciennik A, Burdett V, Modrich PL. DNA mismatch repair: functions and mechanisms. Chemical reviews. 2006; 106:302–323. [PubMed: 16464007]

Johnson RE, Kovvali GK, Guzder SN, Amin NS, Holm C, Habraken Y, Sung P, Prakash L, Prakash S. Evidence for involvement of yeast proliferating cell nuclear antigen in DNA mismatch repair. The Journal of biological chemistry. 1996; 271:27987–27990. [PubMed: 8910404]

Kadyrov FA, Dzantiev L, Constantin N, Modrich P. Endonucleolytic function of MutLalpha in human mismatch repair. Cell. 2006; 126:297–308. [PubMed: 16873062]

Kadyrov FA, Genschel J, Fang Y, Penland E, Edelmann W, Modrich P. A possible mechanism for exonuclease 1-independent eukaryotic mismatch repair. Proceedings of the National Academy of Sciences of the United States of America. 2009; 106:8495–8500. [PubMed: 19420220]

Kadyrov FA, Holmes SF, Arana ME, Lukianova OA, O'Donnell M, Kunkel TA, Modrich P. Saccharomyces cerevisiae MutLalpha is a mismatch repair endonuclease. The Journal of biological chemistry. 2007; 282:37181–37190. [PubMed: 17951253]

Kane MF, Loda M, Gaida GM, Lipman J, Mishra R, Goldman H, Jessup JM, Kolodner R. Methylation of the hMLH1 promoter correlates with lack of expression of hMLH1 in sporadic colon tumors and mismatch repair-defective human tumor cell lines. Cancer research. 1997; 57:808–811. [PubMed: 9041175]

Kastrinos F, Stoffel EM. The History, Genetics, and Strategies for Cancer Prevention in Lynch Syndrome. Clinical gastroenterology and hepatology: the official clinical practice journal of the American Gastroenterological Association. 2013

Kolodner RD, Marsischky GT. Eukaryotic DNA mismatch repair. Current opinion in genetics & development. 1999; 9:89–96. [PubMed: 10072354]

Krishna TS, Kong XP, Gary S, Burgers PM, Kuriyan J. Crystal structure of the eukaryotic DNA polymerase processivity factor PCNA. Cell. 1994; 79:1233–1243. [PubMed: 8001157]

Lau PJ, Flores-Rozas H, Kolodner RD. Isolation and characterization of new proliferating cell nuclear antigen (POL30) mutator mutants that are defective in DNA mismatch repair. Molecular and cellular biology. 2002; 22:6669–6680. [PubMed: 12215524]

Li F, Mao G, Tong D, Huang J, Gu L, Yang W, Li GM. The histone mark H3K36me3 regulates human DNA mismatch repair through its interaction with MutSalpha. Cell. 2013; 153:590–600. [PubMed: 23622243]

Li GM. Mechanisms and functions of DNA mismatch repair. Cell research. 2008; 18:85–98. [PubMed: 18157157]

Liberti SE, Larrea AA, Kunkel TA. Exonuclease 1 preferentially repairs mismatches generated by DNA polymerase alpha. DNA repair. 2013; 12:92–96. [PubMed: 23245696]

Lin YL, Shivji MK, Chen C, Kolodner R, Wood RD, Dutta A. The evolutionarily conserved zinc finger motif in the largest subunit of human replication protein A is required for DNA replication and mismatch repair but not for nucleotide excision repair. The Journal of biological chemistry. 1998; 273:1453–1461. [PubMed: 9430682]

Liu Y, Kadyrov FA, Modrich P. PARP-1 enhances the mismatch-dependence of 5′-directed excision in human mismatch repair in vitro. DNA repair. 2011; 10:1145–1153. [PubMed: 21945626]

Longley MJ, Pierce AJ, Modrich P. DNA polymerase delta is required for human mismatch repair in vitro. The Journal of biological chemistry. 1997; 272:10917–10921. [PubMed: 9099749]

Marsischky GT, Filosi N, Kane MF, Kolodner R. Redundancy of Saccharomyces cerevisiae MSH3 and MSH6 in MSH2-dependent mismatch repair. Genes & development. 1996; 10:407–420. [PubMed: 8600025]

Palombo F, Iaccarino I, Nakajima E, Ikejima M, Shimada T, Jiricny J. hMutSbeta, a heterodimer of hMSH2 and hMSH3, binds to insertion/deletion loops in DNA. Current biology: CB. 1996; 6:1181–1184. [PubMed: 8805365]

Peltomaki P. Role of DNA mismatch repair defects in the pathogenesis of human cancer. J Clin Oncol. 2003; 21:1174–1179. [PubMed: 12637487]

Peltomaki P, Vasen HF. Mutations predisposing to hereditary nonpolyposis colorectal cancer: database and results of a collaborative study. The International Collaborative Group on Hereditary Nonpolyposis Colorectal Cancer. Gastroenterology. 1997; 113:1146–1158. [PubMed: 9322509]

Pluciennik A, Dzantiev L, Iyer RR, Constantin N, Kadyrov FA, Modrich P. PCNA function in the activation and strand direction of MutLalpha endonuclease in mismatch repair. Proceedings of the National Academy of Sciences of the United States of America. 2010; 107:16066–16071. [PubMed: 20713735]

Prelich G, Tan CK, Kostura M, Mathews MB, So AG, Downey KM, Stillman B. Functional identity of proliferating cell nuclear antigen and a DNA polymerase-delta auxiliary protein. Nature. 1987; 326:517–520. [PubMed: 2882424]

Prolla TA, Pang Q, Alani E, Kolodner RD, Liskay RM. MLH1, PMS1, and MSH2 interactions during the initiation of DNA mismatch repair in yeast. Science (New York, NY. 1994; 265:1091–1093.

Shell SS, Putnam CD, Kolodner RD. The N terminus of Saccharomyces cerevisiae Msh6 is an unstructured tether to PCNA. Molecular cell. 2007; 26:565–578. [PubMed: 17531814]

Sia EA, Kokoska RJ, Dominska M, Greenwell P, Petes TD. Microsatellite instability in yeast: dependence on repeat unit size and DNA mismatch repair genes. Molecular and cellular biology. 1997; 17:2851–2858. [PubMed: 9111357]

Smith CE, Mendillo ML, Bowen N, Hombauer H, Campbell CS, Desai A, Putnam CD, Kolodner RD. Dominant Mutations in S. cerevisiae PMS1 Identify the Mlh1-Pms1 Endonuclease Active Site and an Exonuclease 1-Independent Mismatch Repair Pathway. PLoS genetics. 2013; 9:e1003869. [PubMed: 24204293]

Srivatsan A, Bowen N, Kolodner RD. Mispair-specific Recruitment of the Mlh1-Pms1 Complex Identifies Repair Substrates of the Saccharomyces cerevisiae Msh2-Msh3 Complex. The Journal of biological chemistry. 2014; 289:9352–9364. [PubMed: 24550389]

The Cancer Genome Atlas Network. Comprehensive molecular characterization of human colon and rectal cancer. Nature. 2012; 487:330–337. [PubMed: 22810696]

Tishkoff DX, Amin NS, Viars CS, Arden KC, Kolodner RD. Identification of a human gene encoding a homologue of Saccharomyces cerevisiae EXO1, an exonuclease implicated in mismatch repair and recombination. Cancer research. 1998; 58:5027–5031. [PubMed: 9823303]

Tishkoff DX, Boerger AL, Bertrand P, Filosi N, Gaida GM, Kane MF, Kolodner RD. Identification and characterization of Saccharomyces cerevisiae EXO1, a gene encoding an exonuclease that interacts with MSH2. Proceedings of the National Academy of Sciences of the United States of America. 1997; 94:7487–7492. [PubMed: 9207118]

Tran HT, Gordenin DA, Resnick MA. The 3′-->5′ exonucleases of DNA polymerases delta and epsilon and the 5′-->3′ exonuclease Exo1 have major roles in postreplication mutation avoidance in Saccharomyces cerevisiae. Molecular and cellular biology. 1999; 19:2000–2007. [PubMed: 10022887]

Tran PT, Simon JA, Liskay RM. Interactions of Exo1p with components of MutLalpha in Saccharomyces cerevisiae. Proceedings of the National Academy of Sciences of the United States of America. 2001; 98:9760–9765. [PubMed: 11481425]

Umar A, Buermeyer AB, Simon JA, Thomas DC, Clark AB, Liskay RM, Kunkel TA. Requirement for PCNA in DNA mismatch repair at a step preceding DNA resynthesis. Cell. 1996; 87:65–73. [PubMed: 8858149]

Vijayakumar S, Chapados BR, Schmidt KH, Kolodner RD, Tainer JA, Tomkinson AE. The C-terminal domain of yeast PCNA is required for physical and functional interactions with Cdc9 DNA ligase. Nucleic acids research. 2007; 35:1624–1637. [PubMed: 17308348]

Wei K, Clark AB, Wong E, Kane MF, Mazur DJ, Parris T, Kolas NK, Russell R, Hou H Jr, Kneitz B, et al. Inactivation of Exonuclease 1 in mice results in DNA mismatch repair defects, increased cancer susceptibility, and male and female sterility. Genes & development. 2003; 17:603–614. [PubMed: 12629043]

Xie Y, Counter C, Alani E. Characterization of the repeat-tract instability and mutator phenotypes conferred by a Tn3 insertion in RFC1, the large subunit of the yeast clamp loader. Genetics. 1999; 151:499–509. [PubMed: 9927446]

Yuan F, Gu L, Guo S, Wang C, Li GM. Evidence for involvement of HMGB1 protein in human DNA mismatch repair. The Journal of biological chemistry. 2004; 279:20935–20940. [PubMed: 15014079]

Zhang Y, Yuan F, Presnell SR, Tian K, Gao Y, Tomkinson AE, Gu L, Li GM. Reconstitution of 5′-directed human mismatch repair in a purified system. Cell. 2005; 122:693–705. [PubMed: 16143102]

Zhou Y, Hingorani MM. Impact of individual proliferating cell nuclear antigen-DNA contacts on clamp loading and function on DNA. The Journal of biological chemistry. 2012; 287:35370–35381. [PubMed: 22902629]

Highlights

- PCNA mutants disrupt Exo1-independent MMR by two mechanisms

- Mutants either poorly bind Msh2-Msh6 or poorly activate the Mlh1-Pms1 endonuclease

- Activation mutations are enhanced by loss of the interaction with Msh2-Msh6

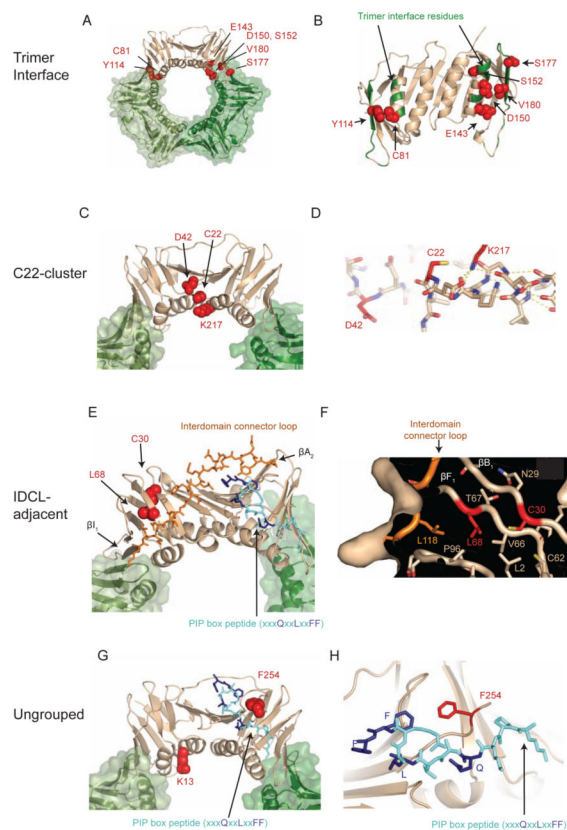- Msh2-Msh6 promotes excision by localizing PCNA for Mlh1-Pms1 activation

Figure 1. *pol30* mutations that disrupt Exo1-independent MMR cause amino acid changes that form clusters on the PCNA crystal structure

(A–B) The positions of amino acids altered by trimer interface mutations. (A) Mutated amino acids are depicted as red spheres on the tan subunit in the PCNA trimer. (B) Rotated view of the PCNA monomer displays mutated residues as red spheres. Other non-mutated trimer interface residues are colored green on the backbone ribbon. (C–D) The positions of amino acids altered by the C22-cluster mutations. (C) Displayed as in (A). (D) The K217 side chain (red) caps the C-terminus of the αA_1 helix by hydrogen bond interactions with backbone carbonyls (dashed yellow lines) and may help position C22 (red). (E–F) The positions of the amino acids altered in the IDLC-adjacent mutations. (E) Displayed as in (A) with the IDCL as orange sticks and the PIP-box peptide as blue sticks, with conserved residues as dark blue. Positions of the two β-sheets (βI_1 and βA_2) at either end of the IDCL are labelled. (F) Cutaway surface depiction shows part of the hydrophobic core containing L68 and C30 that pack with residues of the IDCL and another β-sheet that interacts with the adjacent PCNA protomer. (G–H) The positions of the amino acids altered in the unclustered mutations. (G) Displayed as in (A) with the PIP-box peptide as blue sticks, with conserved residues as dark blue. (H) Position of the F254 side chain (red sticks) relative to the PIP-box peptide (blue sticks). PCNA and PCNA/PIP-box peptide structures rendered using PDB entries 1plq and 2od8 (Krishna et al., 1994; Vijayakumar et al., 2007). Also see Figure S1.
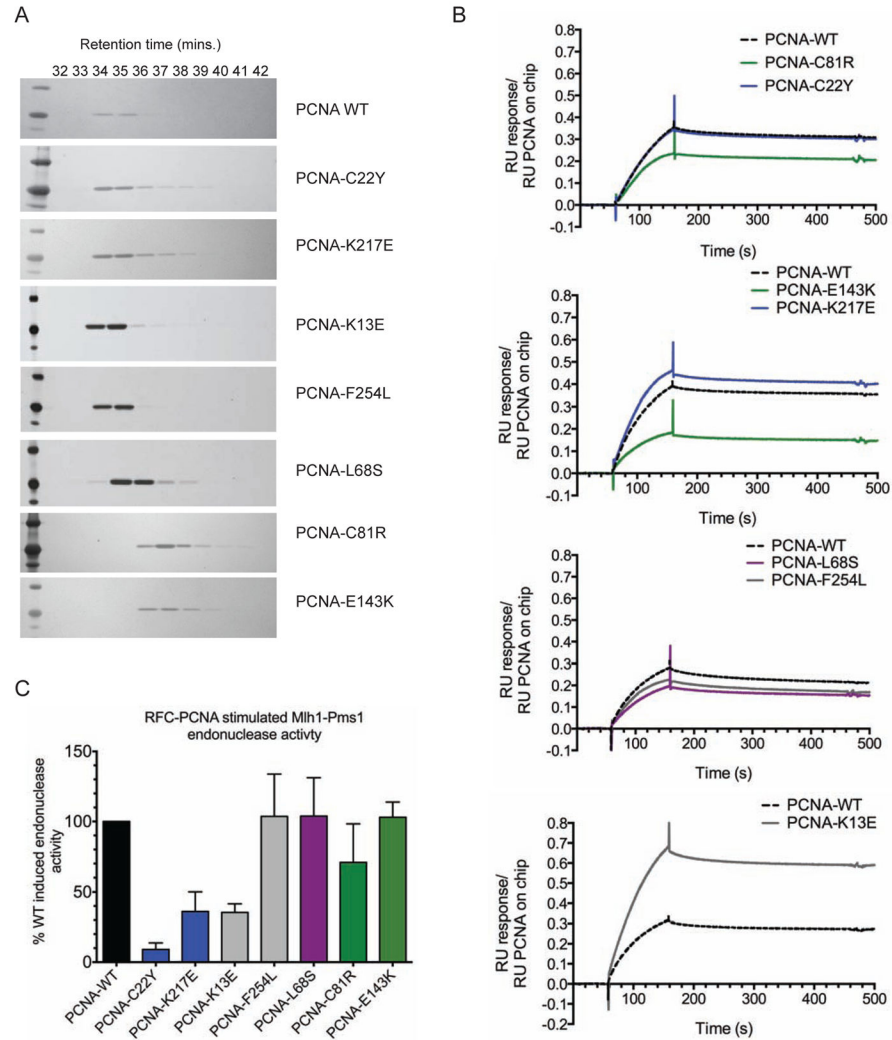
Figure 2. Biochemical characterization of PCNA mutant proteins
(A) Purified mutant PCNA proteins were chromatographed on a size exclusion column and analyzed by SDS-PAGE. (B) Msh2-Msh6 binding to wild-type or mutant PCNA was analysed by SPR. PCNA was bound to the chip and RU was monitored over a 100 s injection of 100 nM Msh2-Msh6 followed by 300 s of buffer flow. Data is normalized to the amount of biotinylated PCNA in each channel and the sensorgrams from representative experiments are shown. Mutants are shown in relation to the wild-type control performed on each chip (dotted black line) and colored according to their grouping on the PCNA crystal structure (blue- C22Y-cluster, green- trimer interface, purple- IDCL-adjacent, grey-ungrouped). Also see Figure S3. (C) Activation of the Mlh1-Pms1 endonuclease by wild-type and mutant PCNA. Purified Mlh1-Pms1 was incubated with RFC and either wild-type or mutant PCNA along with supercoiled circular DNA. The percentage of the nicked product produced relative to that produced by Mlh1-Pms1, RFC and wild-type PCNA was determined. The value presented is the average (+/− standard deviation) from replicate experiments.
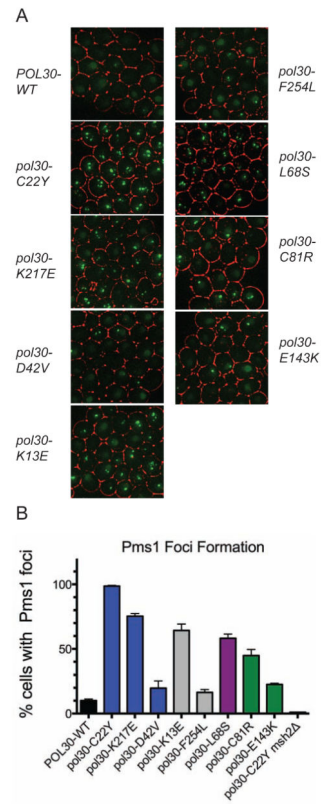
Figure 3. MMR intermediates accumulate in cells containing *pol30* mutations
(A) Representative images of Mlh1-Pms1-4xGFP foci for strains containing the indicated *pol30* allele imaged from logarithmically growing asynchronous cultures. (B) Fraction of cells with Pms1 foci for the wild-type and indicated *pol30* mutants. The average value (+/− standard deviation) for 2 or more independent experiments is presented.

Mispair recognition by Msh2-Msh6

Msh2-Msh6

RFC   PCNA

impaired by
msh6 PIP-box mutations

Residual PCNA from replication
Or
Recruitment/retention of PCNA by Msh2-Msh6

impaired by
pol30 Msh6-interaction mutations

Mlh1-Pms1

Recruitment of Mlh1-Pms1

pms1 endonuclease
mutations

slowed by pol30
nuclease activation mutants

DNA nicking by Mlh1-Pms1

Exo1-Independent   **Exo1-Dependent**

heterozygous *pms1*
endonuclease mutations

pol30 nuclease activation mutants

failure to retain PCNA by Msh6   ⊢ *exo1Δ*

Additional rounds of DNA nicking by Mlh1-Pms1 (slow)   Recruitment of and cleavage by Exo1 (fast)

Exo1

Template for strand resynthesis

Figure 4. Impact of mutations on Exo1-independent and Exo1-dependent MMR pathways
Mutations in MMR genes either inhibit (red) or impair (yellow) common steps in Exo1-independent or Exo1-dependent MMR as well as steps that are specific to Exo1-independent MMR. Recognition of mispairs by Msh2-Msh6 and recruitment of Mlh1-Pms1 by Msh2-Msh6 are steps common to both MMR pathways and are required for the formation of the Mlh1-Pms1 foci MMR intermediates. At least an initial PCNA-activated endonuclease cleavage event by Mlh1-Pms1 is required for both downstream pathways. The activating PCNA could either be retained on the newly replicated DNA or loaded at a nick by RFC (Hombauer et al., 2011a; Pluciennik et al., 2010). When the Exo1-dependent pathway is inactivated, mutations that partially reduce the activation of Mlh1-Pms1, including

mutations that disrupt the localization of PCNA by Msh2-Msh6, cause large increases in mutation rates due to a potential requirement for multiple cleavage events by Mlh1-Pms1. When the Exo1-dependent pathway is functional, mutations that partially reduce the activation of Mlh1-Pms1 cause much smaller increases in mutation rates because the Exo1-dependent pathway may not require multiple cleavage events by Mlh1-Pms1. Although loss of the Exo1-independent pathway only causes a minor increase in mutation rates in the presence of Exo1, loss of this pathway causes increased Mlh1-Pms1 foci, suggesting that the Exo1-dependent pathway has slower kinetics of processing MMR intermediates when activation of Mlh1-Pms1 is partially reduced. Because both leading and lagging strand replication leave nicks in the DNA as well as sites where PCNA might remain after completion of DNA synthesis (Discussed in (Hombauer et al., 2011b)). The repair of both leading and lagging strands generated during DNA replication seems likely to involve similar mechanisms.

Table 1

Summary of *pol30* mutator mutations studied.

Allele[*]	Mutator phenotype (plasmid)	*Complemented by EXO1*	Mutator phenotype (integrated)	Base substitution(s)
Trimer interface				
pol30-C81R (pol30-204)	+	+	High	c.241T>C
pol30-Y114H (pol30-207)	+	+	n.d.	c.340T>C
pol30-E143K[**]	+	+	Medium	c.427G>A
pol30-D150E[**]	+	+	Low	c.450C>G
pol30-S152P	+	+	Medium	c.454T>C
pol30-S177P (pol30-212)	+	+	n.d.	c.529T>C
pol30-V180D[**]	+	+	Medium	c.539T>A
C22-cluster				
pol30-C22Y[**] (*pol30-201*)	+	+	High	c.65G>A
pol30-D42V	+	+	Low	c.125A>T
pol30-K217E	+	+	High	c.649A>G
IDLC-adjacent				
pol30-C30R	+	_ψ	Low	c.88T>C
pol30-L68S[**]	+	+	High	c.203T>C
Unclustered				
pol30-K13E[**] (*pol30-114*)	+	+	Medium	c.37A>G
pol30-F254L[**]	+	+	Low	c.760T>C
Not *exo1* specific				
pol30-K13E,L50S,F144L	+	–	n.d.	c.37A>G, c.149T>C, c.430T>C
pol30-V23A	+	–	n.d.	c.68T>A
pol30-S49P (pol30-202)	+	–	n.d.	c.145T>C
pol30-F207S,K217E	+	–	n.d.	c.620T>C, c.649A>G
pol30-S222P	+	–	n.d.	c.664T>C
Multiple mutations				
pol30-C22Y,D93G	+	+	n.d.	c.65G>A, c.278A>G
pol30-L68S,S145P	+	+	n.d.	c.203T>C, c.433T>C
pol30-T73I,V180D	+	+	n.d.	c.218C>T, c.539T>A
pol30-D120V,K217E	+	+	n.d.	c.359A>T, c.649A>G
pol30-D134G,D150E	+	+	n.d.	c.401A>G, c.450C>G
pol30-I181V,F254L	+	+	n.d.	c.541A>G, c.760T >C
Not mutators				
pol30-L50S[**]	–	n.d.	n.d.	c.149T>C
pol30-T73I[**]	–	n.d.	n.d.	c.218C>T
pol30-D93G[**]	–	n.d.	n.d.	c.278A>G
pol30-D120V[**]	–	n.d.	n.d.	c.359A>T
pol30-D134G[**]	–	n.d.	n.d.	c.401A>G

Allele[*]	Mutator phenotype (plasmid)	*Complemented by EXO1*	Mutator phenotype (integrated)	Base substitution(s)
pol30-F144L[**]	–	n.d.	n.d.	c.430T>C
pol30-S145P[**]	–	n.d.	n.d.	c.433T>C
pol30-I181V[**]	–	n.d.	n.d.	c.541A>G

n.d. = not determined.

[*] allele names specify the amino acid change. Names in parenthesis are previous allele names when isolated from independent screens (Chen et al., 1999; Lau et al., 2002).

[**] alleles created by site directed mutagenesis to separate out mutations observed in alleles containing multiple amino acid substitutions with the exception of *pol30-E143K*, which was generated because it was isolated in a previous screen (Amin et al., 2001).

[ψ]Complementation of the mutator phenotype by *EXO1* was observed with the plasmid allele but was not observed with the integrated allele. Also see Tables S1 and S2 and Figure S2.

Table 2

Mutation rates caused by *pol30* mutations at the *POL30* genomic locus.

Genotype	*hom3-10* Reversion Rate	*lys2-10A* Reversion Rate	Can^R Mutation Rate
Wild-type	2.26 [1.22–3.30] ×10^{-9} (1)	1.01 [0.67–1.86] ×10^{-8} (1)	5.65 [3.56–8.53] × 10^{-8} (1)
msh2	3.96 [2.48–5.34] × 10^{-6} (1,752)	7.48 [3.89–8.27] × 10^{-5} (7,405)	4.77 [3.19–13.9] × 10^{-6} (84)
exo1	4.93 [3.04–10.2] × 10^{-9} (2)	4.02 [2.67–7.34] × 10^{-8} (4)	2.58 [1.52–11.2] × 10^{-7} (5)
exo1 msh2	4.74 [3.21–5.16] × 10^{-6} (2,097)	7.32 [4.77–15.0] × 10^{-5} (7,248)	3.14 [2.66–3.84] × 10^{-6} (56)
pol30-E143K	5.38 [4.17–10.5] × 10^{-9} (2)	2.14 [1.33–2.86] × 10^{-7} (21)	9.94 [7.37–20.0] × 10^{-8} (1.8)
pol30-E143K exo1	8.76 [4.97–12.4] × 10^{-8} (39)	4.93 [3.92–7.04] × 10^{-6} (488)	7.32 [4.61–10.1] × 10^{-7} (13)
pol30-E143K msh2	4.68 [3.79–5.74] × 10^{-6} (2,070)	1.20 [0.83–2.62] × 10^{-4} (11,881)	3.24 [1.71–5.15] × 10^{-6} (57)
pol30-C81R	2.56 [1.72–6.41] × 10^{-7} (113)	1.09 [0.63–1.51] × 10^{-5} (1,079)	4.40 [2.16–7.12] × 10^{-7} (8)
pol30-C81R exo1	1.81 [1.21–3.29] × 10^{-6} (800)	4.29 [3.27–6.13] × 10^{-5} (4,247)	3.46 [2.01–5.06] × 10^{-6} (61)
pol30-S152P	1.40 [0.82–2.57] × 10^{-8} (6)	7.22 [4.37–2.54] × 10^{-7} (71)	2.52 [2.19–5.98] × 10^{-7} (4)
pol30-S152P exo1	1.76 [1.36–3.36] × 10^{-7} (78)	8.05 [6.50–17.1] × 10^{-6} (797)	2.26 [1.33–3.82] × 10^{-6} (40)
pol30-S152P msh2	5.55 [4.27–7.70] × 10^{-6} (2,456)	9.69 [6.39–15.9] × 10^{-5} (9,594)	5.18 [4.11–7.22] × 10^{-6} (92)
pol30-C22Y	2.34 [0.57–3.83] × 10^{-7} (104)	1.57 [1.08–1.80] × 10^{-5} (1,554)	6.19 [3.76–7.81] × 10^{-7} (11)
pol30-C22Y exo1	2.44 [1.85–3.18] × 10^{-6} (1,079)	3.47 [1.78–9.43] × 10^{-5} (3,436)	4.71 [3.80–11.6] × 10^{-6} (83)
pol30-K217E	9.27 [7.47–18.0] × 10^{-9} (4)	3.26 [2.39–5.33] × 10^{-7} (32)	3.99 [3.43–5.98] × 10^{-7} (7)
pol30-K217E exo1	1.66 [1.39–3.54] × 10^{-6} (735)	4.04 [2.80–5.94] × 10^{-5} (4,000)	4.76 [3.53–7.48] × 10^{-6} (84)
pol30-K217E msh2	6.75 [5.63–12.4] × 10^{-6} (2,987)	8.70 [6.70–12.3] × 10^{-5} (8,614)	6.68 [5.70–12.0] × 10^{-6} (118)
pol30-D42V	1.96 [1.51–2.68] × 10^{-9} (0.9)	1.82 [1.55–2.59] × 10^{-8} (1.8)	7.26 [6.04–10.4] × 10^{-8} (1.3)
pol30-D42V exo1	1.34 [0.84–1.82] × 10^{-8} (6)	1.20 [0.77–1.87] × 10^{-6} (119)	5.19 [4.22–6.86] × 10^{-7} (9)
pol30-D42V msh2	3.32 [2.89–4.69] × 10^{-6} (1,469)	8.80 [5.36–12.4] × 10^{-5} (8,713)	3.31 [2.10–5.16] × 10^{-6} (59)
pol30-K13E	5.69 [3.11–9.28] × 10^{-9} (2.5)	1.61 [1.21–2.33] × 10^{-7} (16)	3.10 [2.52–4.99] × 10^{-7} (5)
pol30-K13E exo1	3.65 [2.21–5.24] × 10^{-7} (162)	9.43 [5.44–13.7] × 10^{-6} (933)	1.21 [0.91–1.82] × 10^{-6} (21)
pol30-K13E msh2	5.97 [4.82–8.81] × 10^{-6} (2,642)	1.41 [0.73–2.24] × 10^{-4} (13,960)	6.50 [3.86–10.3] × 10^{-6} (115)
pol30-F254L	2.83 [1.39–3.20] × 10^{-9} (1.3)	3.50 [2.26–4.85] × 10^{-8} (3.5)	9.76 [7.89–11.8] × 10^{-8} (1.7)
pol30-F254L exo1	3.11 [1.74–7.42] × 10^{-8} (14)	3.32 [1.44–5.75] × 10^{-6} (329)	9.59 [4.38–19.3] × 10^{-7} (17)
pol30-F254L msh2	7.47 [5.53–12.1] × 10^{-6} (3,305)	1.50 [0.74–2.67] × 10^{-4} (14,851)	5.14 [4.69–14.3] × 10^{-6} (91)
pol30-L68S	4.31 [2.74–6.50] × 10^{-8} (19)	8.43 [7.14–10.8] × 10^{-7} (83)	5.00 [3.79–8.67] × 10^{-7} (9)
pol30-L68S exo1	5.62 [4.18–8.40] × 10^{-7} (249)	1.61 [1.22–2.39] × 10^{-5} (1,594)	3.41 [2.60–.21] × 10^{-6} (61)
pol30-L68S msh2	4.38 [3.48–5.45] × 10^{-6} (1,938)	6.79 [4.52–8.13] × 10^{-5} (6,723)	4.92 [4.03–6.48] × 10^{-6} (87)

Reported rates are the median rates with 95% confidence interval in square brackets. Fold increase in mutation rate over the wild-type strain rate (RDKY5964) is listed in parenthesis. Total loss of mismatch repair is represented by *msh2* (RKDY8263). Also see Figures S4 and S5.

Table 3

Mutation rates caused by *pol30* mutations in the *msh6 2-50 msh3* double mutant.

Genotype	*hom3-10* Reversion Rate	*lys2-10A* Reversion Rate	Can^R Mutation Rate
Wild-type			
alone	$2.26\ [1.22–3.30] \times 10^{-9}$ (1)	$1.01\ [0.67–1.86] \times 10^{-8}$ (1)	$5.65\ [3.56–8.53] \times 10^{-8}$ (1)
msh6 2-50 msh3	$3.47\ [2.70–6.77] \times 10^{-7}$ (154)	$1.15\ [0.73–2.99] \times 10^{-6}$ (114)	$4.57\ [2.52–6.24] \times 10^{-7}$ (8)
pol30-E143K			
alone	$5.38\ [4.17–10.5] \times 10^{-9}$ (2)	$2.14\ [1.33–2.86] \times 10^{-7}$ (21)	$9.94\ [7.37–20.0] \times 10^{-8}$ (1.8)
msh6 2-50 msh3	$9.60\ [6.25–13.7] \times 10^{-7}$ (425)	$5.30\ [3.47–5.59] \times 10^{-6}$ (525)	$5.99\ [4.35–7.79] \times 10^{-7}$ (11)
pol30-K217E			
alone	$9.27\ [7.47–18.0] \times 10^{-9}$ (4)	$3.26\ [2.39–5.33] \times 10^{-7}$ (32)	$3.99\ [3.43–5.98] \times 10^{-7}$ (7)
msh6 2-50 msh3	$3.20\ [2.6–4.38] \times 10^{-6}$ (1,416)	$2.16\ [1.74–3.50] \times 10^{-5}$ (2,139)	$1.93\ [1.52–2.41] \times 10^{-6}$ (34)
pol30-K13E			
alone	$5.69\ [3.11–9.28] \times 10^{-9}$ (2.5)	$1.61\ [1.21–2.33] \times 10^{-7}$ (16)	$3.10\ [2.52–4.99] \times 10^{-7}$ (5)
msh6 2-50 msh3	$1.95\ [1.46–2.64] \times 10^{-6}$ (863)	$1.35\ [0.71–1.74] \times 10^{-5}$ (1,337)	$1.27\ [1.13–1.66] \times 10^{-6}$ (22)
pol30-F254L			
alone	$2.83\ [1.39–3.20] \times 10^{-9}$ (1.3)	$3.50\ [2.26–4.85] \times 10^{-8}$ (3.5)	$9.76\ [7.89–11.8] \times 10^{-8}$ (1.7)
msh6 2-50 msh3	$4.59\ [3.46–6.07] \times 10^{-7}$ (203)	$2.46\ [1.67–3.6] \times 10^{-6}$ (244)	$4.57\ [3.79–7.39] \times 10^{-7}$ (8)
pol30-L68S			
alone	$4.31\ [2.74–6.50] \times 10^{-8}$ (19)	$8.43\ [7.14–10.8] \times 10^{-7}$ (83)	$5.00\ [3.79–8.67] \times 10^{-7}$ (9)
msh6 2-50 msh3	$1.51\ [1.21–2.32] \times 10^{-6}$ (668)	$9.69\ [7.42–14.4] \times 10^{-6}$ (959)	$1.78\ [1.10–2.46] \times 10^{-6}$ (32)

Reported rates are the median rates with 95% confidence interval in square brackets. Fold increase in mutation rate over the wild-type strain rate (RDKY5964) is listed in parenthesis.